



# The relationship between fire severity and burning efficiency for estimating wildfire emissions in Mediterranean forests

Bountouraby Balde<sup>1</sup> · Cristina Vega-García<sup>1</sup> ·  
Pere Joan Gelabert<sup>1</sup> · Aitor Ameztegui<sup>1</sup> ·  
Marcos Rodrigues<sup>2</sup>

Received: 14 June 2022 / Accepted: 24 November 2022  
© The Author(s) 2023

**Abstract** Forests are exposed to changing climatic conditions reflected by increasing drought and heat waves that increase the risk of wildfire ignition and spread. Climatic variables such as rain and wind as well as vegetation structure, land configuration and forest management practices are all factors that determine the burning potential of wildfires. The assessment of emissions released by vegetation combustion is essential for determining greenhouse gases and air pollutants. The estimation of wildfire-related emissions depends on factors such as the type and fraction of fuel (i.e., live biomass, ground litter, dead wood) consumed by the fire in a given area, termed the burning efficiency. Most approaches estimate live burning efficiency from optical remote sensing data. This study used a data-driven method to estimate live burning efficiency in a Mediterranean area. Burning severity estimations from Landsat imagery (dNBR), which relate to fuel consumption, and quantitative field data from three national forest inventory data were combined to

establish the relationship between burning severity and live burning efficiency. Several proxies explored these relationships based on dNBR interval classes, as well as regression models. The correlation results between live burning efficiency and dNBR for conifers ( $R=0.63$ ) and broad-leaved vegetation ( $R=0.95$ ) indicated ways for improving emissions estimations. Median estimations by severity class (low, moderate-low, moderate-high, and high) are provided for conifers (0.44–0.81) and broad-leaves (0.64–0.86), and regression models for the live fraction of the tree canopy susceptible to burning (<2 cm, 2–7 cm, >7 branches, and leaves). The live burning efficiency values by severity class were higher than previous studies.

**Keywords** Forest wildfires · Emissions · Greenhouse gases · Satellite images

## Introduction

Wildfires burn hundreds of thousands of hectares in the Mediterranean Basin annually (Ganteaume et al. 2013). Depopulation and rural exodus occurring since the 1950s, with abandonment of traditional forest management and accompanying forest densification and expansion, have resulted in fuel buildup and continuity that have led to higher intensity fires with increased destruction (Bodí et al. 2012). Beyond the loss in biodiversity and damaged habitats, wildfires can contribute a large and highly variable fraction of biomass emissions (Collier et al. 2016). Biomass combustion releases greenhouse gases (GHG) (Zavala et al. 2014), that contribute to global warming (Whelan 1995). Depending on the type of fuel burnt, other gases such as carbon monoxide, methane, and nitric oxide may be released (Castillo et al. 2003; Balde and Vega-García 2019). These gases contribute

---

Project funding: This work was partially funded by project FIREPATHS (PID2020-116556RA-I00), supported by the Spanish Ministry of Science and Innovation, and by project CLIMARK (LIFE16 CCM/ES/000065, supported by the LIFE Climate Change Mitigation EU program). Bountouraby Balde received a predoctoral grant from the University of Lleida.

---

The online version is available at <http://www.springerlink.com>

---

Corresponding editor: Yu Lei.

---

✉ Bountouraby Balde  
bountouraby.balde@udl.cat

<sup>1</sup> Department of Agriculture and Forest Engineering, University of Lleida, , Av. Alcalde Rovira Roure, 191, 25198 Lleida, Spain

<sup>2</sup> Department of Geography and Land Management, University of Zaragoza, Pedro Cerbuna 12, 50009 Saragossa, Spain

to air pollution and health-related impacts on people (Liu et al. 2015; Williamson et al. 2016). To date, there are a number of inventories that estimate CO<sub>2</sub> output from wildfires worldwide, mostly based on remote sensing imagery, burned area and burning efficiency estimations (Wiedinmyer et al. 2011; Giglio et al. 2013). The most common estimations relies on moderate resolution sensors (e.g., MODIS) and the greenhouse gases observing satellite (GOSAT) (Ross et al. 2013; Guo et al. 2015; Guo 2020). However, recent developments highlight limitations in these approaches due to the inability to capture the actual contribution of small-sized fires (van der Werf et al. 2017).

Spatial differences in fire frequency, size and intensity result in widely variable socioecological impacts (Viegas et al. 2009). The effects of fires are often gauged as a function of intensity—the amount of energy released by burning—or severity—the level of damage caused (Bodí et al. 2012). For instance, fire intensity has been extensively used to estimate tree mortality rates or damage to buildings (Stephens et al. 2018), while severity has been related to the fraction of biomass consumed (De Santis et al. 2010b; Turetsky et al. 2011; Kukavskaya et al. 2014; Murphy et al. 2019). Within any burned area, different levels of fire severity can be found, depending on fire behaviour (Oliva 2013). The estimation of severity for the assessment of fire effects has commonly relied on spectral indices from remote sensing imagery; both the normalized burn ratio (NBR) and the delta normalized burn ratio (dNBR) have often been used (Fernández-Manso and Quintano 2015; Stambaugh et al. 2015; Chu et al. 2016; Warner et al. 2017; Fernández-García et al. 2018a; Parks et al. 2018; García-Llamas et al. 2019; Lotufo et al. 2020). Fire severity assessments are linked to the amount of biomass and organic matter consumed in the combustion process (Davies et al. 2016), usually defined in relative terms (adimensional) (Pausas 2012; Oliva 2013). Changes in fire severity are related to large differences in the amount of fuel consumed during the fire. Therefore, knowledge of both the degree of fire damage (severity) and the amount of pre-fire fuel consumed is essential to improve emissions estimates (Conard and Solomon 2008). Fuel consumption can proceed at variable rates during a wildfire, so an estimation of the fraction of the total fuel potentially available that is actually burned must be considered as a spatial and temporal dynamic variable related to the severity level (Oliva 2013). An incorrect estimation of this burned fraction can result in large errors (from 23 to 46%) in the quantification of emissions from wildfires (De Santis et al. 2010b), since fire emissions are typically estimated as the product of burned area, fuel load, burned fraction and a specific emission factor (g kg<sup>-1</sup> of dry matter burned) (Urbanski 2014).

Previous work has designated the fraction of available biomass or fuel consumed as *burning efficiency* (Seiler and

Crutzen 1980), *combustion completeness* (van der Werf et al. 2017) or *combustion factor* (Akagi et al. 2011), with similar and dimensionless definitions (Oliva 2013). In this study, the percentage or fraction of available biomass or fuel consumed by fire in a specific area is referred to as *burning efficiency* (BE) (De Santis et al. (2010a). Methods for the estimation of BE can be grouped in two categories: (1) those based on field measurements (Araújo et al. 1999; Fearnside et al. 2001; Righi et al. 2009); and, (2) those based on spectral changes in the vegetation caused by biomass burning (Wiedinmyer et al. 2006; De Santis et al. 2010b; der Werf et al. 2010; Garcia et al. 2017); both estimate fuel consumption from the state of the vegetation before and after a fire. There is still no standard method to perform field-based estimations, partly due to the wide range of factors that may be considered (Chuvieco et al. 2006). These kinds of studies are usually restricted to prescribed fires, which do not experience the range of severities of an unplanned wildfire. The Intergovernmental Panel on Climate Change (IPCC) Tier 3, state-of-the art level (EEA 2019), assimilates vegetation types to the National Fire Danger Rating System fuel types (Deeming et al. 1977): each of the five components of the fuel types (live, dead fine, dead small, dead large, duff) are assigned a specific burning efficiency and emission factor depending on their flaming or smoldering combustion, which is related to the diameter of the fuel component (Leenhouts 1998; Köble et al. 2008a). However, the level of uncertainty is large (EEA 2019), and the number of fuel types to fit all cases small (Köble et al. 2008a). Remote sensing methods currently prevail because of the continuous technical improvements in spectral, spatial, and temporal resolution, good coverage, and the expense and effort required by field surveys using field data only for validation. While these methods have been valuable in global, national and regional estimations, the remaining uncertainties related to the quantification of consumed fuel require exploring other approaches (Ellicott et al. 2009). Burning efficiency has been the main cause of divergences when estimating smoke emissions (Ottmar et al. 2009), Knorr et al. 2012) since fuel consumption varies with fuel types and their components. Ottmar et al. (2009) further indicated that not only vegetation types but both prescribed and wildfire fires need to be considered for more accurate emissions estimations due to their different severities.

In this study, a methodology combining national forest inventory (NFI) data and burn severity estimates was developed to calibrate the live fraction of the canopies, which is the fraction estimated from RS methods through spectral changes. This method builds upon the Spanish National Forest Inventory programme which provides detailed forest inventory data since the 1970s. It provides the necessary allometric information to estimate live standing biomass (LSB) at the stand level. The long NFI data available

on those plots affected by wildfire were used to estimate the fraction of live biomass loss, or live burning efficiency (LBE). LBE was then linked to burn severity estimations via Landsat imagery (dNBR) to produce empirical LBE-dNBR relationships. Traditionally, emission estimates assume an average value of BE for all fuel components of each fuel type, considering the total standing biomass which is inaccurate. The reality of different severity levels occurring within any fire make it evident that BE should be a dynamic and compounded factor (Oliva 2020), in which relationship to each component must be considered separately.

The novelty of our proposal lies in the focus on the live fraction which may account for 10–48% of the total biomass consumed (estimated from forest classes in Table 3, (Köble et al. 2008b), and the use of three consecutive NFI records (NFI2, 1990s; NFI3, 2000s; and NFI4, 2010s) to characterize and spatialize standing live biomass fuel consumption. Live burning efficiency was derived from forest structural changes in plots affected by various severity levels in several Mediterranean forest types in NE Spain, a region in which such studies are lacking despite high fire incidence. Burning efficiencies have been estimated in some studies (De Santis et al. 2010b; Garcia et al. 2017) for Mediterranean-type climate zones in California. In comparison, in the Mediterranean area of Europe, where intense summer fires with increasing frequencies are often uncontrolled (Evyugina et al. 2014), there is a scarcity of studies on BE (De Santis et al. 2010b). To our knowledge, only Oliva and Chuvieco (2011) have performed this type of study in a European Mediterranean area (Spain).

## Materials and methods

The methodology was implemented in four steps: (1) all plots affected by fires larger than 50 ha between the 2<sup>nd</sup> and 4<sup>th</sup> NFI surveys were identified (1992 to 2016); (2) live standing biomass (branches plus leaves) was calculated using the algometric equations from Montero et al. (2005); (3) the burn severity at plot level was determined based on the perimeters of those fires affecting NFI plots and the Normalized Burn Ratio (dNBR) was calculated using Landsat imagery; and, (4) the differences between biomass in each plot was calculated using the closest NFI survey before and after fire to output the LBE factor and model severity-LBE relationships.

## Study area

This study was in Catalonia, a fire-prone region in NE Spain. Catalonia covers 32,108 km<sup>2</sup> (Fig. 1) of which forests are approximately 60% (Cervera et al. 2015). The predominant climate is Mediterranean, with mild winters and dry and

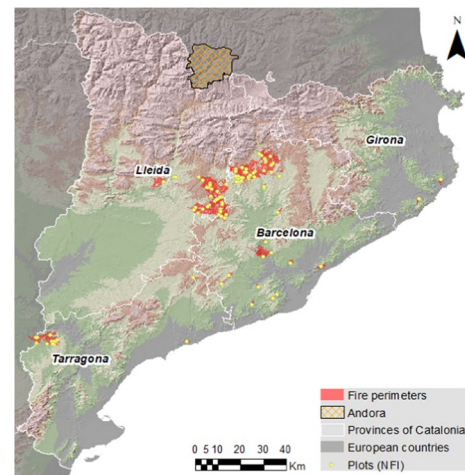


**Fig. 1** Study area and location of NFI plots affected by fires in 1986–2016

warm summers; mean temperatures oscillate between 0 °C and 17 °C, and annual precipitation between 400 and 1200 mm. The region has complex mosaics of agricultural lands intermingling with shrubs and trees on abandoned marginal land. Species diversity is high and rich in endemics (Fady-Welterlen 2005), with Aleppo pine (*Pinus halepensis* Mill.) predominant in the lowlands, replaced with altitude by black pine (*Pinus nigra* Arn), Scots pine (*Pinus sylvestris* L.) and mountain pine (*Pinus uncinata* Ram.), irregularly and locally mixed with *Quercus* spp., beech (*Fagus sylvatica* L.), chestnut (*Castanea sativa* Mill.), and other species.

The region is frequently subject to forest fires (González-Olabarria et al. 2015), although in terms of area burned, it generally aggregates in the extreme northeast, as well as in the interior of the central zone and the southwest (Rodríguez et al. 2019). An annual average of 650 fires are recorded, burning around 11.5 thousand ha, and most of these fires are human-caused, starting near urban settlements or roads (González-Olabarria et al. 2015).

## Forest inventory data

All available forest field survey data on forests structure and composition in fire-affected plots in the period 1986–2016 were used. The study period spanned the last three national forest inventories (NFI2, NFI3 and NFI4). The Spanish NFI creates a permanent network of plots using a regular sampling strategy at the intersections of a 1 km × 1 km UTM grid established over digital maps (1: 25,000) and revisited every 10 years. Each plot consists of four concentric fixed circles with radii of 5, 10, 15 and 25 m and used for the acquisition of stand and site variables (Alberdi et al. 2014). Plots affected by fires in the period 1986–2016 were selected to match dates between fires (pre-fire and post-fire data) and

NFI surveys; fire perimeters were retrieved from the GenCat repository (<http://agricultura.gencat.cat>; (Table 1). A total of 60 plots surveyed 3–7 years after a fire were selected. Plots sampled less than two years after a fire event were excluded since they were not properly measured (e.g., most trees were

considered dead and no information was retrieved). These plots were affected by 22 fires larger than 50 ha, many of which occurred in 1994. The largest (Casserres) burned 22,243.2 ha (Table 1). Pre-fire vegetation was mainly composed of pine (*Pinus halepensis*, *Pinus sylvestris*) and evergreen Holm oak (*Quercus ilex* L.) forest types (Table 2). As the number of plots was related to the frequency with which fires burn a community type and the area it occupies, in this study there were more plots of conifers than of broad-leaved species.

**Table 1** List of fires in the study area, date of occurrence, and total area burnt

Fires	Date of occurrence	Total area burnt (ha)
Casserres	04/07/1994	22,243.2
Aguilar de Segarra	18/07/1998	15,272.3
Cardona	19/07/1998	8668.0
La Pobla de Massaluca	14/09/1994	6508.3
Collbató	04/07/1994	3164.8
Ponts	23/08/1994	2542.8
Badalona	11/08/1994	688.7
Mediona	10/08/1994	405.5
Forallac	16/03/2014	380.2
Terrassa	04/07/1994	345.5
Castellbell i el Vilar	21/08/1994	334.9
Santa Cristina d'Aro	09/03/2012	328.5
Olivella	29/07/2000	291.3
Calders	01/07/1994	288.7
Pontils	10/04/1994	261.1
Torrelles de Llobregat	08/07/1995	238.1
Prats de Lluçanès	23/08/1994	231.6
Torrelles de Foix	20/07/1994	158.8
Bassella	18/07/1998	157.1
Gaià	22/06/1998	146.4
Tarragona	09/07/1995	145.3
Subirats	07/04/1994	103.7

### Estimation of standing live biomass

The estimation of standing biomass of the live potentially burnable fractions of the crowns for the 60 plots was determined using the algometric equations by Montero et al. (2005), which relate total dry biomass or some of the tree fractions (t) with normal diameter (dbh) (Eq. 1). The live burnable biomass fractions of the individual trees (leaves and branches up to 7 cm) were added to provide total plot values in t/ha.

$$\text{Tree biomass} = CF * e^a * dbh^b * N * 10000 \quad (1)$$

where CF is a corrective coefficient ( $CF = e^{SEE^2/2}$ ) of the standard error of the estimation (SEE),  $e$  Euler's number,  $dbh$  the diameter at breast high in cm,  $a$  and  $b$  are model constants that depend on the species, and  $N$  is the number of trees. Scarce species in the plots with similar structure to the predominant ones were assimilated to these (e.g., *Quercus pubescens* Willd.) and *Quercus petraea* Liebl.) were estimated with the same equation as *Quercus ilex*; Table 3).

**Table 2** Forest types with number of plots, mean diameter (dm) and mean height (Hm)

Forest type	No plots	dm (cm)	Hm (m)
<i>Pinus sylvestris</i> forests	11	16.8	9.7
Mixed autochthonous broadleaves and coniferous forest of the Mediterranean biogeographical region	10	17.1	6.4
<i>Quercus ilex</i> forests	9	27.4	7.9
<i>Pinus halepensis</i> forests	9	23.3	8.3
<i>Pinus pinaster</i> Ait. forests	3	18.6	7.8
Birch forests	3	22.1	7.7
Mixed autochthonous broadleaved and coniferous forest of the Alpine biogeographical region	3	27.6	12.6
Riparian forests	2	13.8	6.8
<i>Pinus nigra</i> forests	2	16.3	5.8
Fir forests	2	20.9	13.5
Mixed autochthonous broadleaved forest of the Alpine biogeographical region	2	20.5	8.9
Mixed coniferous forest of the Mediterranean biogeographical region	1	20.4	7.4
Mixed broadleaves forest of the Mediterranean biogeographical region	1	17.9	8.9
Mixed autochthonous coniferous forest of the Alpine biogeographical region	1	20.5	9.7
Beech forests	1	24.5	8.3



**Table 3** Function parameters  $\beta_0$  and  $\beta_1$  for biomass estimation and standard error (SEE) according to Montero et al. (2005)

Species	Symbols	$\beta_1$	$\beta_0$	SEE
<i>Pinus halepensis</i>	BR <sub>7</sub>	-9.550	3.611	0.926
	BR <sub>2-7</sub>	-4.727	2.335	0.413
	BR <sub>2</sub>	-2.745	2.037	0.226
<i>Pinus sylvestris</i>	BR <sub>7</sub>	-15.047	4.804	0.816
	BR <sub>2-7</sub>	-4.079	2.141	0.721
	BR <sub>2</sub>	-2.084	1.510	0.625
<i>Pinus nigra</i>	BR <sub>7</sub>	-13.810	4.632	0.958
	BR <sub>2-7</sub>	-6.625	2.925	0.527
	BR <sub>2</sub>	-2.835	2.045	0.211
<i>Pinus pinaster</i>	BR <sub>7</sub>	-23.042	6.524	0.324
	BR <sub>2-7</sub>	-6.663	2.639	0.744
	BR <sub>2</sub>	-4.667	2.380	0.528
<i>Pinus pinea</i>	BR <sub>7</sub>	-4.337	2.600	0.537

BR<sub>7</sub> = biomass of branches with diameters > 7 cm, BR<sub>2-7</sub> = biomass of branches with diameters between 2 and 7 cm, BR<sub>2</sub> = biomass of branches with diameters < 2 cm, BA = biomass of needles, BH = biomass of leaves; scarce species with similar tree structure were assimilated to these species

### Estimation of burn severity in NFI plots

Burn severity levels were estimated from Landsat imagery using the *delta of the Normalized Burn Ratio* (dNBR; (Key and Benson 2006). dNBR is calculated is the difference observed in the normalized burn ratio (NBR), an index specifically designed to identify burnt areas. Similar to the NDVI, the NBR is a normalized index that combines near infrared and short wave infrared wavelengths (NIR and SWIR between 0.7 y 1.3 μm and 1.3 y 2.5 μm, respectively) bands (Wang et al. 2009) (Eq. 2).

$$NBR = (NIR - SWIR)/(NIR + SWIR) \quad (2)$$

where NIR = near infrared, SWIR = short wave infrared wavelengths.

The values of the dNBR for pixels in the plots were classified according to the standard burn severity interval classes of the United States Geological Survey (Key and Benson 2006). The normalized burn ratio is positive in areas with intense photosynthetic activity and negative in areas with low plant productivity or without vegetation. To discriminate burned from unburned areas and provide a quantitative measure of the change in the area, the post-fire NBR is subtracted from the pre-fire NBR, producing the dNBR index. The index is multiplied by 103 to get a continuous range of values between < -0.25 and 1.30. Negative values are usually the result of the presence of clouds in the pre-fire image or rapid plant regeneration (herbaceous) in the post-fire image (< -0.25 < dNBR < -0.1). The positive

**Table 4** Burn Severity Classes from (Key and Benson 2006)

Burn Severity	dNBR
High post-fire regrowth	< -0.25
Low post-fire regrowth	-0.25 to -0.1
Unburned	-0.1 to +0.1
Low-severity burn	+0.1 to +0.27
Moderate-low severity burn	+0.27 to +0.44
Moderate-high severity burn	+0.44 to +0.66
High-severity burn	+0.66 to +1.30

values (between 0.1 and 1.30) are produced by the degree of impact of the fire on the vegetation and the soil, which can be categorized into different classes of severity (Table 4). Both raw dNBR and burn severity classes were linked to NFI plots. All plots were located at least at 30 m inside fire scars, thus dNBR values come from fully burnt pixels. Landsat imagery (TM and ETM+ sensors) and dNBR calculations were performed using the Google Earth Engine platform. Pre- and post-fire NBR were calculated for all fires affecting NFI plots using the Tier 1 Surface Reflectance product.

### Estimation of plot-level live burning efficiencies (LBE<sub>i</sub>)

Plot-level live burning efficiencies (LBE<sub>i</sub>) were calculated as the ratio between the standing biomass before and after the fire, according to Eq. 3.

$$LBE_i = Bio_{pre} - Bio_{post}/Bio_{pre} \quad (3)$$

where: LBE<sub>i</sub> is the live burning efficiency, *Bio<sub>pre</sub>* the live potentially burnable biomass measured before the fire (pre-IFN computed value), *Bio<sub>post</sub>* the biomass measured after fire (post-IFN computed value).

### Analysis of the relation between severity and standing living biomass consumption

A summary of the values in the plots was produced, reflecting the before and after living burnable biomass load, dNBR and LBE<sub>i</sub> for the species grouped for analysis based on structural characteristics. The relation between LBE<sub>i</sub> and burn severity class was determined using three methods. First, a simple exploratory correlation analysis was applied; secondly, the average value of LBE<sub>i</sub> based on dNBR classes was calculated (Table 4); thirdly, empirical relationships were modelled via log-linear regression.

### Estimations based on dNBR classes

To determine the LBE<sub>i</sub> according to burn severity intervals, plots were split according to the four burn severity classes

in Table 4 (dNBR > 0.1; low, moderate-low, moderate-high, high). For each severity class reported, an averaged LBE value was calculated as the mean of all plots in the same severity class. Complementary central (median) and dispersion (standard deviation, sd), quartiles and interquartile range (IQR) statistics were also reported. To assess the degree of similarity of the observed LBE, significant inter-class differences were tested using the Dunn's/Kruskal Wallis test for a rank classification, a non-parametric test suitable when testing more than two independent groups. The Bonferroni method was used for the correction of the significance level.

### Estimations based in regression models

A log-linear regression model was fitted to calibrate the relationship between unclassified dNBR values and LBE. A regression model in which LBE acted as response variable and dNBR was the sole predictor was trained and tested. The performance of the prediction was evaluated by implementing a leave-one-out cross-validation (LOOCV) procedure. The LOOCV consists of an iterative procedure where a model is trained with all observations but one, which is used to evaluate its predictive ability. This process is repeated as until each record has intervened once in the validation.

Performance was summarized as the Pearson's R square coefficient.

### Results

The results from the 60 plots analyzed indicated that the two species most often affected by fire were *Pinus halepensis* and *Pinus nigra* (44 plots). Values found in the estimation of the compounded burnable fractions of live biomass (+ 7 cm branches, 2–7 cm branches, branches < 2 and leaves) are presented in Table 5. Severity and consumption were higher for the oak species than for the pines.

The correlation analysis suggested a fair degree of association between LBE and dNBR. The Pearson correlation coefficient showed a strong log-linear association between plot-BE<sub>i</sub> values and severity (dNBR) by species and globally (R = 0.68). The correlations were statistically significant ( $p < 0.05$ ), with correlation coefficients R 0.63 in conifers, and 0.95 in broadleaves (Fig. 2).

### Estimations of LBE based on burn severity classes

Conifers sustained all severity levels, while broadleaves started moderately low as the lower severity occurrence. This suggests that conifers experience the full range of burn

**Table 5** Summary of biomass (t/ha), dNBR mean according to number of plots and species grouped as conifers and broadleaves)

Dominant Species	Species grouped	N° Plots	Biomass Before	Biomass After	Median dNBR	IQR dNBR	Mean dNBR	sd dNBR
<i>Pinus halepensis</i> ; <i>Pinus pinaster</i> ; <i>Pinus pinea</i> ; <i>Pinus nigra</i> ; <i>Pinus sylvestris</i>	Conifers	49	42.9	13.5	0.56	0.36	0.53	0.21
<i>Quercus ilex</i> ; <i>Quercus pubescens</i> ; <i>Quercus petraea</i>	Broadleaves	11	39.88	9.28	0.71	0.3	0.67	0.27

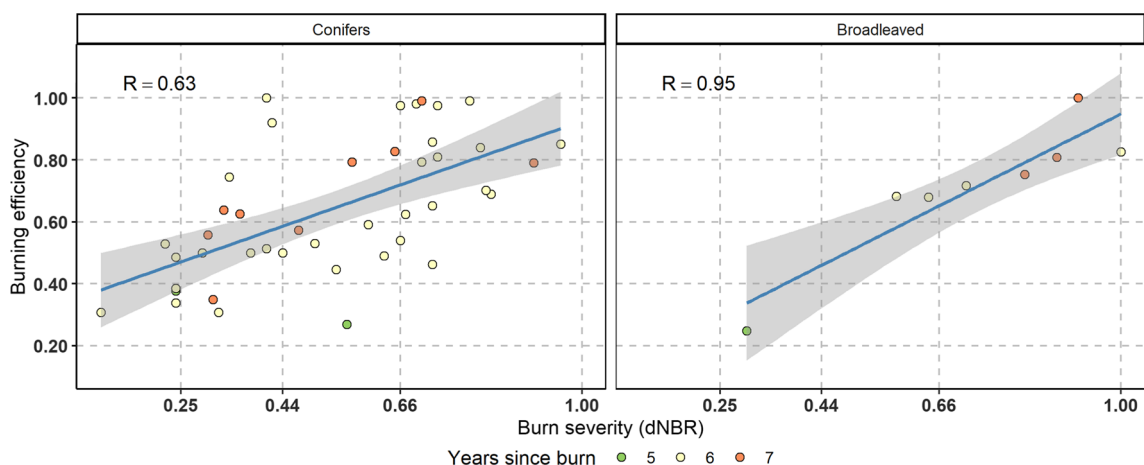


**Fig. 2** Linear association between plot-LBE<sub>i</sub> and dNBR, by species group

**Table 6** Summary of LBEs values according to standard dNBR interval classes by species grouped as conifers and broadleaves

Severity class	N	Species	Mean	Median	IQR	sd
Low	15	Conifers	0.429	0.440	0.150	0.138
Moderate-low	7	Conifers	0.597	0.550	0.095	0.083
Moderate-high	4	Conifers	0.600	0.605	0.135	0.138
High	23	Conifers	0.777	0.810	0.245	0.166
Moderate-low	3	Broadleaves	0.645	0.645	0.195	0.276
Moderate-high	1	Broadleaves	0.840	0.840	0.000	NA
High	7	Broadleaves	0.825	0.860	0.085	0.122

N is the number of plots, IQR is the quartiles and interquartile range, sd is the standard deviation

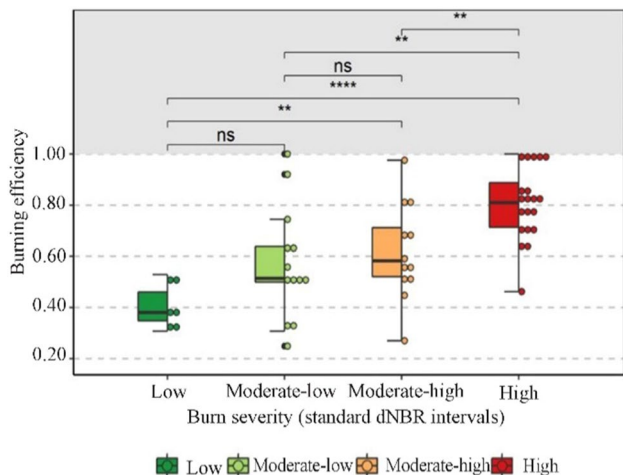


**Fig. 3** Distribution of the plot-BEi across standard intervals of severity; brackets indicate pairwise comparison and significance level according to the Kruskal–Wallis test. ns,  $P > 0.05$ ; \*\*,  $P < 0.01$ ; \*\*\*\*,  $P < 0.0001$

severities possible in the Mediterranean environment but not the broadleaved species. Significant differences between mean and median LBE values were not found; median values are typically less susceptible to extreme values or outliers, so LBE values computed as median were selected for the pairwise comparison in the Kruskal–Wallis test. The differences in LBE median values between all severity classes was significant according to the Dunn’s/Kruskal Wallis test for rank classification (Kruskal–Wallis  $P < 0.05$ ). The median values of LBE in conifers increased with severity class (low = 0.44, moderate-low = 0.55, moderate-high = 0.60 and high = 0.81). The increment was significant between the moderate-high (0.60) and high (0.81) classes. The broadleaved species showed a similarity between the median LBE values for moderate-high = 0.84 and high = 0.86, but the increase in value between the moderate-low (0.64) and moderate-high (0.84) classes was significant (Table 6; Fig. 3).

The standard deviation of LBE values showed higher dispersion in the moderate classes, but IQR displayed a higher variability in the moderate-high and high severity classes

**Table 7** Summary of LBE values according to standard dNBR interval classes by all species

Severity class	N	Mean	Median	IQR	sd
Low	15	0.404	0.381	0.113	0.086
Moderate-low	13	0.569	0.514	0.138	0.221
Moderate-high	12	0.617	0.582	0.190	0.189
High	20	0.806	0.809	0.174	0.142

N is the number of plots, IQR is the quartiles and interquartile range, sd is the standard deviation

(Table 7). Values reflect the trend of fires in the study area towards the higher spectrum of severity.

### Estimations based in regression models

The Pearson’s correlation coefficient (0.68, above) pointed to a dependency relation between LBE and dNBR which led to the fitting of a predictive model. The log-linear model fitted to predict LBE from dNBR for conifers and broadleaves is described in Eqs. 4 and 5 for  $dNBR < 1$ . Where  $dNBR > 1$ , Eq. 6 is applied to both conifers and broadleaves. Given that the log-linear fit can predict values over 1, which would mean a total consumption of biomass (100%), predicted values over the threshold  $dNBR > 0.66$  matching high-severity burning, the maximum in the study by Key and Benson (2006) were also assigned value 1. The goodness of fit of the predicted regression estimated by the coefficient of determination on observed and predicted values was  $R^2 \approx 0.46$  for conifers (Fig. 4) and  $R^2 \approx 0.41$  for broadleaves (Fig. 5). A slight underestimation of LBE was detected, especially in plots affected by high severity fires (high dNBR).

Despite the relatively low value of the coefficient of determination, it can be accepted from the results that it is possible to estimate LBE as a function of dNBR, since all coefficients in the log-linear regression were significant according to the Fisher test ( $F; p < 0.05$ ). The Durbin-Watson test revealed no autocorrelation in our data (statistic  $DW = 1.92$  and  $p\text{-value} = 0.688$ ).

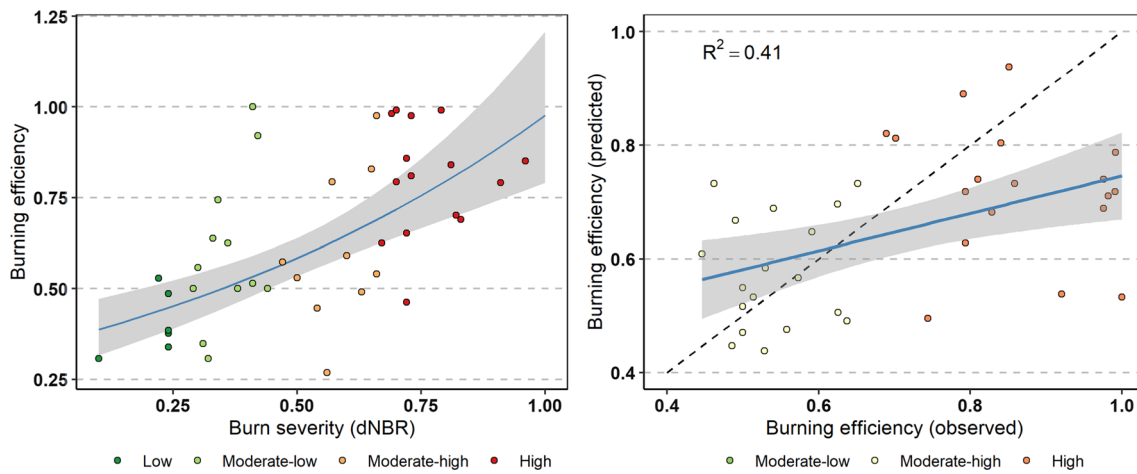


**Fig. 4** Goodness-of-fit of the log linear model for plot-LBEi and severity (dNBR). Left: relation severity-LBE; right: comparison LBE observed-predicted (conifers)

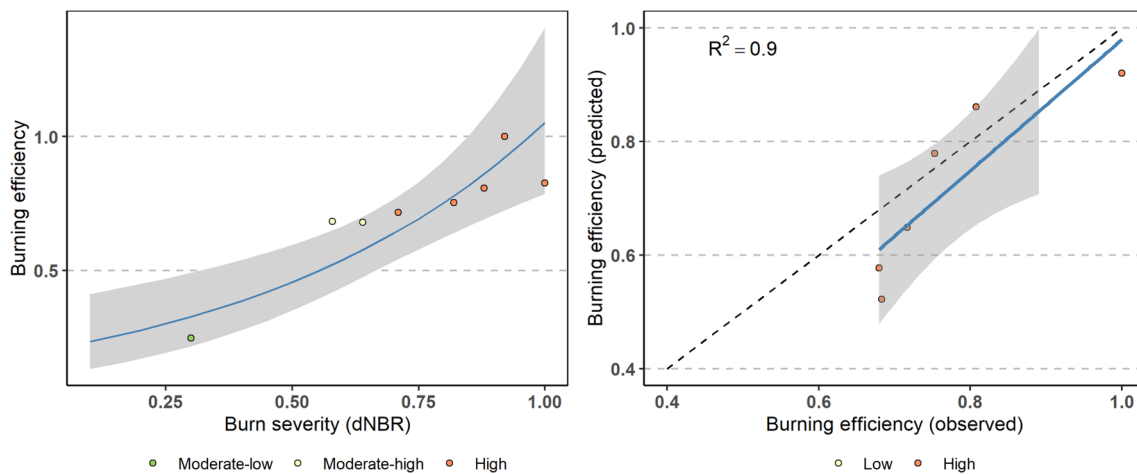


**Fig. 5** Goodness-of-fit of the log linear model for plot-LBEi and severity (dNBR). Left: relation severity-LBE; right: comparison LBE observed-predicted (broadleaves)

$$dNBR < 1.0 \rightarrow LBE = e^{1.029dNBR-1.052} \quad (4)$$

$$dNBR < 1.0 \rightarrow LBE = e^{1.669dNBR-1.618} \quad (5)$$

$$dNBR > 1.0 \rightarrow LBE = 1 \quad (6)$$

## Discussion

dNBR was used to estimate fire severity was a good indicator over other severity indices such as RdNBR and CBI (Composite Burn Index) (Cocke et al. 2005; Hudak et al. 2007; Soverel et al. 2010). Our dNBR analysis indicated

that most plots belonged in the moderate-high and high severities classes (Fig. 3), in agreement with findings by Fernández-García et al. (2018b) and Saulino et al. (2020) in Mediterranean areas. Severity levels from moderate to high are common within burned areas in this region (De Santis et al. 2010a), as also reported in this study.

Live burning efficiencies (LBE) were derived from the changes in live standing biomass estimated in NFI plots in a Mediterranean region exposed to high fire incidence and low to high severities. Recent studies on burning efficiency have increasingly relied on remote sensing data but have been limited in their calibration and validation of relationships by scarce field data due generally to budget constraints. Numerous environmental monitoring programs often face similar constraints and have had to rely on ongoing inventories



(Smith et al. 2013). The use of NFI plot data overcomes this limitation for forest vegetation, as these data are routinely and extensively by national forestry bodies. NFIs apply precise and systematic statistical methods to the estimation of forest characteristics and consider spatial changes in stand structure (Barrett and Gray 2011). They save field time and funds and have proved valuable over the last decades for many natural resource applications (Corona et al. 2011). Tailored field measurements in a range of vegetation types might allow for more accurate estimations of LBE (live burning efficiency) but they are not easily acquired and cannot be timely programmed to before and after a fire that is not prescribed. The particular conditions of sampling and then burned were not common in our study area; the number of plots that met the requirements were sixty. While enough for exploring dNBR-LBE relations and model development at this stage, widening the study area could provide more plots for more species to analyze, provided fire incidence is similar.

The available national forest inventory data did not provide quantitative information on all burned fuel fractions, only the standing biomass of the tree crowns. In Mediterranean environments, the understorey vegetation (shrubs, herbs) can be burned almost completely, depending on fire severity (Cadena et al. 2020), but these fractions are not estimated in NFI plots. Additionally, no data is available, at least in Spanish NFI, for estimation of the fuel load of dead woody material and duff components which have their own specific burning efficiencies and emission factors, depending on their flaming or smoldering combustion, related to the diameter of the fuel component (Leenhouts 1998).

This indicates that our approach specifically provides burning efficiencies for the live fraction of the standing biomass in forests, excluding the understorey. Nevertheless, the overstorey is the part of the forest vegetation remotely sensed by most passive sensors for Earth observation (Carreiras et al. 2006). While this is also true in all previous work that have used the vegetation channels for burning efficiency estimations, it must be noted that consumption and emission estimations may be largely underestimated by considering only the live fraction of the top vegetation layer, or assuming it is the largest contributor. According to our estimation from Table 3 in Köble et al. (2008b), the live fraction burned may account for only 10–48% of the total forest biomass consumed (33% on average).

While this study may be limited by data, it is accurate in the definition of the fraction analyzed, which was determined from NFI pre-fire and post-fire biomass in the crown (+ 7 cm branches, 2–7 cm branches, branches < 2 and leaves). However, the largest branches (equivalent to 1000-h lag dead fuels) would only burn under severe conditions, but they are predominant in Mediterranean forests. The use of Montero et al. (2005) formulas added to sources of error to

the estimation of live plot biomass, but in all cases, values were less than 1 t/ha (SEE, Table 3).

The high and significant correlations found between dNBR (normalized burn ratios) and LBE (live burning efficiencies),  $r=0.7$  for conifers and  $r=0.88$  for broadleaves, indicates that these values can be considered very good estimations when used for the forest conditions in NE Spain. Our LBE values by severity class (Table 7, between 0.38 and 0.81) were somewhat higher than those in previous studies, and more discrimination in the medium range of severity (moderate-low, moderate-high) are provided. However, for further studies, it may be possible to expand the sample of plots of low and moderate severity by analyzing prescribed burns with ad hoc inventories, especially for broadleaved species.

Araújo et al. (1999) estimated burning efficiencies for different tree diameters as small-size (5 to 10 cm dbh), medium-size (10 to 30 cm dbh) and large-size (dbh > 30 cm). High burning efficiency values were found for leaves (0.83) and branches (0.61) of small trees (dbh < 10 cm), with a mean of 0.72. Branches for medium and large trees (dbh > 10 cm) had BE values of 0.31. Fearnside et al. (2001) also found similar values to ours in the estimation of biomass for branches, high BE values (0.80) were found for branches with diameters < 5 cm, followed by branches of diameters between 5 and 10 cm (0.52). The lowest value was for branches with diameters > 10 cm (0.17). They found a decrease in burning efficiency with an increase in size of tree components, as expected, but they did not consider different severity levels and nor species. It has been common in previous studies for BE to be applied as an average value to a full wildfire and to all species present, but our results show that the variability in severity and species type should be considered.

Oliva and Chuvieco (2011) estimated burning efficiencies in another area in Spain and established three burning efficiency values by vegetation type and level of damage. For conifers, they reported the following: low severity (0.25), medium (0.42) and high (0.57); for broadleaves, values were similar: low (0.25), medium (0.40) and high (0.57). De Santis et al. (2010a) established severity levels and burning efficiencies for three vegetation types: shrubs, broadleaves, and conifers. They adjusted the values based on the burn severity Geo Composite Burn Index (GeoCBI) as: conifers, low (0.25), medium (0.47) and high (0.65); broadleaves: low (0.25), medium (0.40) and high (0.56). These ratios were applied in two very large forest fires in California, in conditions comparable to the ones in our study area, but divergences are possible, given that the geometrically modified Composite Burn Index is a qualitative, visual measure that considers the vegetation fraction cover to determine burn severity of the total plot (De Santis et al. 2009). These researchers did not separate biomass into fractions

or different components for burn efficiency calculations, but beyond considering severity class and species, it would be beneficial to differentiate more fuel fractions by size in future studies, since all tree components do not burn in the same manner. However, future work should consider and standardize the definition of fuel fractions by size, as many studies have used variable size intervals (i.e., 5–10/10–30/+30 cm; <5 cm/5–10/+10 cm; +7 cm/2–7/<2 and leaves), depending on data availability.

The log-linear model was adequate for modelling the relationship dNBR-LBE, beyond the proviso of providing predicted values > 1, which required that they be truncated. Data showed no autocorrelation, and diagnostics were significant. The availability of a model such as this one presents several advantages over ratios by severity classes; we avoid having to average values by categories and provide more accurate quantitative estimations of consumption, hence, also more accurate estimations of emissions. The spatial distribution of consumption can be mapped, and forest recovery actions adjusted more precisely.

## Conclusions

To better characterize the burning efficiencies of wildfires and reduce uncertainties in emissions estimations, it is necessary to consider the different consumptions of live and dead fuels of different sizes, by species, and how they are affected by changing fire severity levels. This study focused on live burning efficiencies and linked national forest inventory biomass data to burn severity estimations via Landsat imagery (dNBR) to produce empirical LBE-dNBR relationships for the live fuel fraction in conifers and broadleaves. Correlations between LBE and dNBR for conifers ( $R=0.63$ ) and broadleaves ( $R=0.95$ ) suggest appropriate LBEs for improving current emissions estimations. Median LBE estimations were provided by severity class (low, moderate-low, moderate-high, and high) for conifers and broadleaves, and regression models for the live fraction of the tree cover susceptible to burning.

Global methods for estimations of fire emissions consider average burning efficiency values for general vegetation types that are assumed to burn partially, but homogeneously. However, large errors can be produced by not considering how species and burn severity influence greenhouse gas emissions, as suggested by our results.

**Funding** Open Access funding provided thanks to the CRUE-CSIC agreement with Springer Nature. This work was partially funded by project FIREPATHS (PID2020-116556RA-I00), supported by the Spanish Ministry of Science and Innovation, and by project CLIMARK (LIFE16 CCM/ES/000065, supported by the LIFE Climate Change

Mitigation EU program). Bountouraby Balde received a predoctoral grant from the University of Lleida.

**Open Access** This article is licensed under a Creative Commons Attribution 4.0 International License, which permits use, sharing, adaptation, distribution and reproduction in any medium or format, as long as you give appropriate credit to the original author(s) and the source, provide a link to the Creative Commons licence, and indicate if changes were made. The images or other third party material in this article are included in the article's Creative Commons licence, unless indicated otherwise in a credit line to the material. If material is not included in the article's Creative Commons licence and your intended use is not permitted by statutory regulation or exceeds the permitted use, you will need to obtain permission directly from the copyright holder. To view a copy of this licence, visit <http://creativecommons.org/licenses/by/4.0/>.

## References

- Akagi SK, Yokelson RJ, Wiedinmyer C, Alvarado MJ, Reid JS, Karl T, Crouse JD, Wennberg PO (2011) Emission factors for open and domestic biomass burning for use in atmospheric models. *Atmos Chem Phys* 11:4039–4072. <https://doi.org/10.5194/acp-11-4039-2011>
- Alberdi I, Cañellas I, Condes S (2014) A long-scale biodiversity monitoring methodology for Spanish national forest inventory. *Appl Álava Region Syst* 23:93–110. <https://doi.org/10.5424/fs/2014231-04238>
- Araújo TM Jr, Carvalho AJ, Higuchi N Jr, Brasil ACP, Mesquita ALA (1999) A tropical rainforest clearing experiment by biomass burning in the state of Pará, Brazil. *Atmos Environ* 33:1991–1998
- Balde B, Vega-García C (2019) Estimación de emisiones de GEI y sus trayectorias en grandes incendios forestales en Cataluña, España. *Madera y Bosques*. <https://doi.org/10.21829/myb.2019.2521764>
- Barrett TM, Gray AN (2011) Potential of a national monitoring program for forests to assess change in high-latitude ecosystems. *Biol Conserv* 144:1285–1294
- Bodí MB, Cerddà A, Mataix-Solera J, Doerr SH (2012) Efectos de los incendios forestales en la vegetación y el suelo en la cuenca mediterránea: Revisión bibliográfica. *Bol la Asoc Geogr Esp* 33–56. <https://doi.org/10.21138/bage.2058>
- Cadena DA, Flores-Garnica JG, Flores-Rodríguez AG, Lomelí-Zavala ME (2020) Efecto de incendios en la vegetación de sotobosque y propiedades químicas de suelo de bosques templados. *Agro Productividad Agro Product* 13:189–198
- Carreiras JM, Pereira JM, Pereira JS (2006) Estimation of tree canopy cover in evergreen oak woodlands using remote sensing. *For Ecol Manage* 223:45–53
- Castillo M, Pedernera P, Pena E (2003) Incendios forestales y medio ambiente: una síntesis global. *Rev Ambient y Desarro* 19:44–53
- Cervera T, Garrabou R, Tello E (2015) Forestry policy and trends in the woodland areas of Catalonia from the 19th century until the present. *Investig Hist Econ* 11:116–127. <https://doi.org/10.1016/j.ih.2014.04.002>
- Chu T, Guo X, Takeda K (2016) Temporal dependence of burn severity assessment in Siberian larch (*Larix sibirica*) forest of northern Mongolia using remotely sensed data. *Int J Wildl Fire* 25:685–698
- Chuvieco E, Riaño D, Danson FM, Martín P (2006) Use of a radiative transfer model to simulate the postfire spectral response to burn severity. *J Geophys Res Biogeosci* 111:1–15. <https://doi.org/10.1029/2005JG000143>
- Cocke AE, Fulé PZ, Crouse JE (2005) Comparison of burn severity assessments using differenced normalized burn ratio and ground

- data. *Int J Wildl Fire* 14:189–198. <https://doi.org/10.1071/WF04010>
- Collier S, Zhou S, Onasch TB, Jaffe DA, Kleinman L, Sedlacek AJ III, Briggs NL, Hee J, Fortner E, Shilling JE, Worsnop D, Yokelson RJ, Parworth C, Ge X, Xu J, Butterfield Z, Chand D, Dubey MK, Pekour MS, Springston S, Zhang Q (2016) Regional influence of aerosol emissions from wildfires driven by combustion efficiency: insights from the BBOP campaign. *Environ Sci Technol* 50:8613–8622
- Conard SG, Solomon AM (2008) Chapter 5 Effects of Wildland Fire on Regional and Global Carbon Stocks in a Changing Environment. *Dev. Environ. Sci.*
- Corona P, Chirici G, McRoberts RE, Winter S, Barbati A (2011) Contribution of large-scale forest inventories to biodiversity assessment and monitoring. *For Ecol Manage* 262:2061–2069
- Davies GM, Domènech R, Gray A, Johnson PCD (2016) Vegetation structure and fire weather influence variation in burn severity and fuel consumption during peatland wildfires. *Biogeosciences* 13:389–398
- De Santis A, Chuvieco E, Vaughan PJ (2009) Short-term assessment of burn severity using the inversion of PROSPECT and GeoSail models. *Remote Sens Environ* 113:126–136. <https://doi.org/10.1016/j.rse.2008.08.008>
- De Santis A, Asner GP, Vaughan PJ, Knapp DE (2010b) Mapping burn severity and burning efficiency in California using simulation models and Landsat imagery. *Remote Sens Environ* 114:1535–1545. <https://doi.org/10.1016/j.rse.2010.02.008>
- Deeming JE, Burgan RE, Cohen JD (1977) The national fire-danger rating system, 1978. Department of Agriculture, Forest Service, Intermountain Forest and Range Experiment Station, vol 39
- der Werf GR, Randerson JT, Giglio L, Collatz GJ, Mu M, Kasibhatla PS, van Leeuwen TT (2010) Global fire emissions and the contribution of deforestation, savanna, forest, agricultural, and peat fires (1997–2009). *Atmos Chem Phys* 10:11707–11735
- EEA (2019) European Union emission inventory report 1990–2017 under the UNECE convention on long-range transboundary air pollution (LRTAP). EEA technical report No 9/2019. Copenhagen: <https://eea.europa.eu/publications/european-union-emissions-inventory-report-2017>. Accessed on 05.03.2022
- Ellicott E, Vermote E, Giglio L, Roberts G (2009) Estimating biomass consumed from fire using MODIS FRE. *Geophys Res Lett* 36:13. <https://doi.org/10.1029/2009GL038581>
- Evtyugina M, Alves C, Calvo A, Nunes T, Tarelho L, Duarte M, Prozil SO, Evtuguin DV, Pio C (2014) VOC emissions from residential combustion of Southern and mid-European woods. *Atmos Environ* 83:90–98. <https://doi.org/10.1016/j.atmosenv.2013.10.050>
- Fady-Welterlen B (2005) Is there really more biodiversity in Mediterranean forest ecosystems? *Taxon* 54:905–910
- Fearnside PM, de Alencastro Graça PML, Rodrigues FJA (2001) Burning of Amazonian rainforests: burning efficiency and charcoal formation in forest cleared for cattle pasture near Manaus, Brazil. *For Ecol Manage* 146:115–128
- Fernández-García V, Santamarta M, Fernández-Manso A, Quintano C, Marcos E, Calvo L (2018a) Burn severity metrics in fire-prone pine ecosystems along a climatic gradient using Landsat imagery. *Remote Sens Environ* 206:205–217
- Fernández-Manso A, Quintano C (2015) Evaluating Landsat ETM+ emissivity-enhanced spectral indices for burn severity discrimination in Mediterranean forest ecosystems. *Remote Sens Lett* 6:302–310
- Ganteaume A, Camia A, Jappiot M, San-Miguel-Ayanz J, Long-Fournel M, Lampin C (2013) A review of the main driving factors of forest fire ignition over Europe. *Environ Manage* 51:651–662. <https://doi.org/10.1007/s00267-012-9961-z>
- García M, Saatchi S, Casas A, Koltunov A, Ustin S, Ramirez C, Balzter H (2017) Quantifying biomass consumption and carbon release from the California Rim fire by integrating airborne LiDAR and Landsat OLI data. *J Geophys Res Biogeosci* 122:340–353
- García-Llamas P, Suárez-Seoane S, Fernández-Guisuraga JM, Fernández-García V, Fernández-Manso A, Quintano C, Taboada A, Marcos E, Calvo L (2019) Evaluation and comparison of Landsat 8, Sentinel-2 and Deimos-1 remote sensing indices for assessing burn severity in Mediterranean fire-prone ecosystems. *Int J Appl Earth Obs Geoinf* 80:137–144. <https://doi.org/10.1016/j.jag.2019.04.006>
- Giglio L, Randerson JT, Van Der Werf GR (2013) Analysis of daily, monthly, and annual burned area using the fourth-generation global fire emissions database (GFED4). *J Geophys Res Biogeosci* 118:317–328. <https://doi.org/10.1002/jgrg.20042>
- González-Olabarria JR, Mola-Yudego B, Coll L (2015) Different factors for different causes: analysis of the spatial aggregations of fire ignitions in Catalonia (Spain). *Risk Anal* 35:1197–1209
- Guo M, Xu J, Wang X, He H, Li J, Wu L (2015) Estimating CO<sub>2</sub> concentration during the growing season from MODIS and GOSAT in East Asia. *Int J Remote Sens* 36:4363–4383
- Guo M (2020) Remote Sensing of CO<sub>2</sub> Emissions from Wildfires. *Terr Ecosyst Biodivers* (p 393–401
- Hudak AT, Morgan P, Bobbitt MJ, Smith AM, Lewis SA, Lentile LB, McKinley RA (2007) The relationship of multispectral satellite imagery to immediate fire effects. *Fire Ecol* 3:64–90
- Key CH, Benson NC (2006) Landscape assessment: remote sensing of severity, the Normalized Burn Ratio. In: Pages LA25--LA41 in DC Lutes. Fire effects monitoring and inventory system. USDA Forest Service, Rocky mountain research station, Fort Collins, Colorado, USA, FIREMON
- Knorr W, Lehsten V, Arneft A (2012) Determinants and predictability of global wildfire emissions. *Atmos Chem Phys* 12:6845–6861. <https://doi.org/10.5194/acp-12-6845-2012>
- Köble R, Barbosa P, Seufert G (2008a) Estimating emissions from vegetation fires in Europe. 2000
- Köble R, Barbosa P, Seufert G (2008b) Estimating emissions from vegetation fires in Europe. *Atmos Environ*, submitted for publication
- Kukavskaya EA, Ivanova GA, Conard SG, McRae DJ, Ivanov VA (2014) Biomass dynamics of central Siberian Scots pine forests following surface fires of varying severity. *Int J Wildl Fire* 23:872–886
- Leenhouts B (1998) Assessment of biomass burning in the conterminous United States. *Conserv Ecol* 2:1
- Liu JC, Pereira G, Uhl SA, Bravo MA, Bell ML (2015) A systematic review of the physical health impacts from non-occupational exposure to wildfire smoke. *Environ Res* 136:120–132
- Lotufo DS, B. J, Machado NG, de Mello Taques, L. de S, M. D, M'utzenberg NLN, Biudes MS, (2020) Índices Espectrais e Temperatura de Superfície em Áreas Queimadas no Parque Estadual do Araguaia em Mato Grosso. *Rev Bras Geogr Física* 13:2
- Montero G, Ruiz-peinado R, Muñoz M (2005) Producción de biomasa y fijación de CO<sub>2</sub> por los bosques españoles
- Murphy BP, Prior LD, Cochrane MA, Williamson GJ, Bowman DM (2019) Biomass consumption by surface fires across Earth's most fire prone continent. *Glob Chang Biol* 25:254–268
- Oliva P, Chuvieco E (2011) Towards a dynamic burning efficiency factor. *Adv Remote Sens GIS Appl For Fire Manag From local to Glob assessments* 47
- Oliva P (2013) FEMM -- Fire Effects Modeling and Mapping: An approach to estimate the spatial variability of burning efficiency. In: en Fernández, D. y Sabia, R. (Coords.): Remote sensing advances for system science the ESA science network: project, pp 93–102. Springer, Berlin, pp 2009–2011
- Oliva P (2020) FEMM—fire effects modelling and mapping : an approach to estimate the spatial variability of burning efficiency

- FEMM—fire effects modelling and mapping : an approach to estimate the spatial variability of burning efficiency. <https://doi.org/10.1007/978-3-642-32521-2>
- Ottmar RD, Miranda AI, Sandberg DV (2009) Characterizing sources of emissions from wildland fires. *Dev Environ Sci* 8:61–78
- Parks SA, Holsinger LM, Voss MA, Loehman RA, Robinson NP (2018) Mean composite fire severity metrics computed with Google Earth Engine offer improved accuracy and expanded mapping potential. *Remote Sens* 10:879
- Pausas JG (2012) Incendios forestales. Editorial CatarataCSIC, Madrid
- Righi CA, de Alencastro Graça LPM, Cerri CC, Feigl BJ, Fearnside PM (2009) Biomass burning in Brazil's Amazonian "arc of deforestation": burning efficiency and charcoal formation in a fire after mechanized clearing at Feliz Natal, Mato Grosso. *For Ecol Manage* 258:2535–2546
- Rodrigues M, Alcasena F, Vega-García C (2019) Modeling initial attack success of wildfire suppression in Catalonia, Spain. *Sci Total Environ* 666:915–927. <https://doi.org/10.1016/j.scitotenv.2019.02.323>
- Ross AN, Wooster MJ, Boesch H, Parker R (2013) First satellite measurements of carbon dioxide and methane emission ratios in wild-fire plumes. *Geophys Res Lett* 40:4098–4102
- De Santis A, Asner GP, Vaughan PJ, Knapp DE (2010a) Mapping burn severity and burning efficiency in California using simulation models and Landsat imagery. *Remote Sens Environ* 114(7):1535–1545. <https://doi.org/10.1016/j.rse.2010a.02.008>
- Saulino L, Rita A, Migliozi A, Maffei C, Allevalo E, Garonna AP, Saracino A (2020) Detecting burn severity across mediterranean forest types by coupling medium-spatial resolution satellite imagery and field data. *Remote Sens* 12:741
- Seiler W, Crutzen PJ (1980) Estimates of gross and net fluxes of carbon between the biosphere and the atmosphere from biomass burning. *Clim Change* 2:207–247. <https://doi.org/10.1007/BF00137988>
- Smith JE, Heath LS, Hoover CM (2013) Carbon factors and models for forest carbon estimates for the 2005–2011 National Greenhouse Gas Inventories of the United States. *For Ecol Manage* 307:7–19
- Soverel NO, Perrakis DD, Coops NC (2010) Estimating burn severity from Landsat dNBR and RdNBR indices across western Canada. *Remote Sens Environ* 114:1896–1909
- Stambaugh MC, Hammer LD, Godfrey R (2015) Performance of burn-severity metrics and classification in oak woodlands and grasslands. *Remote Sens* 7:10501–10522
- Stephens SL, Collins BM, Fettig CJ, Finney MA, Hoffman CM, Knapp EE, Wayman RB (2018) Drought, tree mortality, and wildfire in forests adapted to frequent fire. *Bioscience* 68:77–88
- Turetsky MR, Kane ES, Harden JW, Ottmar RD, Manies KL, Hoy E, Kasischke ES (2011) Recent acceleration of biomass burning and carbon losses in Alaskan forests and peatlands. *Nat Geosci* 4:27–31
- Urbanski S (2014) Wildland fire emissions, carbon, and climate: Emission factors. *For Ecol Manage* 317:51–60
- Viegas DX, Ribeiro LM, Viegas MT, Pita LP, Rossa C (2009) Impacts of fire on society: extreme fire propagation issues. *Earth observation of wildland fires in mediterranean ecosystems*. Springer, Berlin, pp 97–109
- Wang M, Son S, Shi W (2009) Evaluation of MODIS SWIR and NIR-SWIR atmospheric correction algorithms using SeaWiFS data. *Remote Sens Environ* 113:635–644
- Warner TA, Skowronski NS, Gallagher MR (2017) High spatial resolution burn severity mapping of the New Jersey Pine Barrens with WorldView-3 near-infrared and shortwave infrared imagery. *Int J Remote Sens* 38:598–616
- Whelan RJ (1995) *The ecology of fire*. Cambridge University Press, Cambridge
- Wiedinmyer C, Quayle B, Geron C, Belote A, McKenzie D, Zhang X, O'Neill S, Wynne KK (2006) Estimating emissions from fires in North America for air quality modeling. *Atmos Environ* 40:3419–3432. <https://doi.org/10.1016/j.atmosenv.2006.02.010>
- Wiedinmyer C, Akagi SK, Yokelson RJ, Emmons LK, Al-Saadi JA, Orlando JJ, Soja AJ (2011) The fire INventory from NCAR (FINN): a high resolution global model to estimate the emissions from open burning. *Geosci Model Dev* 4:625–641
- Williamson GJ, Bowman DMJS, Price OF, Henderson SB, Johnston FH (2016) A transdisciplinary approach to understanding the health effects of wildfire and prescribed fire smoke regimes. *Environ Res Lett*. <https://doi.org/10.1088/1748-9326/11/12/125009>
- Zavala LM, De Celis R, Jordán A (2014) How wildfires affect soil properties. A brief review. *Cuad Investig Geográfica*; 40:311–332. <https://doi.org/10.18172/cig.2522>
- GRWerfvan derJTRandersonLGiglioTTLeeuwenvanYChenBMRogersMMuMJEMarlevanDCMortonGJCollatzRJYokelsonPSKasibhatla2017Global fire emissions estimates during 1997&2015Earth Syst Sci Data Discuss10.5194/essd-2016-62van der Werf GR, Randerson JT, Giglio L, van Leeuwen TT, Chen Y, Rogers BM, Mu M, van Marle MJE, Morton DC, Collatz GJ, Yokelson RJ, Kasibhatla PS (2017) Global fire emissions estimates during 1997 & 2015. *Earth Syst Sci Data Discuss*. <https://doi.org/10.5194/essd-2016-62>

**Publisher's Note** Springer Nature remains neutral with regard to jurisdictional claims in published maps and institutional affiliations.